Granular Matter (2006) 8: 103–115
DOI 10.1007/s10035-006-0001-7

ORIGINAL PAPER

José María Montanero · Vicente Garzó · Meheboob Alam
Stefan Luding

Rheology of two- and three-dimensional granular mixtures under uniform shear flow: Enskog kinetic theory versus molecular dynamics simulations

Received: 22 July 2005 / Published online: 2 March 2006

Abstract The rheological properties for dilute and moderately dense granular binary mixtures of smooth, inelastic hard disks/spheres under uniform shear flow in steady state conditions are reported. The results are based on the Enskog kinetic theory, numerically solved by a dense gas extension of the Direct Simulation Monte Carlo method for dilute gases. These results are confronted to the ones also obtained by performing molecular dynamics (MD) simulations with good agreement for the lower densities and higher coefficients of restitution. For increasing density and dissipation, the Enskog equation applies qualitatively, but the quantitative differences increase. Possible reasons for deviations of Enskog from MD results are discussed, indicating non-Newtonian flow behavior and anisotropy as the most likely direction in which previous analytical approaches have to be extended.

Keywords Enskog kinetic theory · Dissipative granular gas · Shear flow simulations

J.M. Montanero (✉)
Departamento de Electrónica e Ingeniería Electromecánica,
Universidad de Extremadura,
E-06071 Badajoz, Spain
E-mail: jmm@unex.es

V. Garzó
Departamento de Física,
Universidad de Extremadura,
E-06071 Badajoz, Spain
E-mail: vicenteg@unex.es

M. Alam
Engineering Mechanics Unit,
Jawaharlal Nehru Center (JNCASR),
Jakkur P.O., Bangalore 560064, India
E-mail: meheboob@jncasr.ac.in

S. Luding
Particle Technology,
Nanostructured Materials (NSM)
DelftChem Tech,
Julianalaan 136, 2628 BL Delft, The Netherlands
E-mail: s.luding@tnw.tudelft.nl

1 Introduction

Rapid granular flows can be well modeled by an idealized system of smooth hard disks/spheres with inelastic collisions [1,2]. In addition to an isotropic compression stress, shear (or deviatoric) deformation and stress are present in almost all flow situations. Despite the simplicity of the model, its great advantage is that there is a theory available which applies well in the quasi-elastic, dilute regime. Using this as the starting point, the model was widely studied in the last few years as a prototype to gain some insight into the "microscopic" understanding of physical mechanisms involved in granular flows, and it was step by step extended towards more realistic parameters involving, e.g., size- and mass-disparity, and friction. Understanding the differences between theory and various simulation approaches allows to improve the former, and to identify the relevant set of parameters from the latter. The kinetic theory and, more specifically, the Boltzmann equation for a low density gas [3–6] and the Enskog equation for a moderately dense gas [7,8], are the established theoretical tools to begin with. In recent years, methods have been developed to solve the latter equation and get accurate predictions over a wide range of parameters.

The motivation of this paper is – besides a systematic review and summary of the bi-disperse, dissipative and sheared granular system in *both* two and three dimensions – to show that the theory applies quantitatively well in the low density and low dissipation regime, but that it applies qualitatively still for larger densities, dissipation, and mass-ratios – in both 2D and 3D. After energy non-equipartition is accounted for, and the clustering density instability is avoided, non-Gaussian velocity distributions and the non-Newtonian flow behavior remain as likely reason for discrepancies between otherwise comparable modeling approaches and thus must be understood better.

As said before, for finite higher densities, the Enskog kinetic equation [7,8] can be considered as the extension of the Boltzmann equation. As happens for elastic collisions, the inelastic Enskog equation provides a semiquantitative

description of the hard sphere system that neglects the effects of correlations between the velocities of the two particles that are about to collide (molecular chaos assumption). However, as the system evolves corrections to the Enskog equation due to multiparticle collisions, including recollision events ("ring" collisions) should be incorporated. The latter are expected to be stronger for fluids with inelastic collisions where the colliding pairs tend to be more focused after collision. Therefore, some deviations from molecular chaos have been observed in molecular dynamics (MD) simulations of granular fluids in driven, sheared, or homogeneous states [9–16]. Being not significant for dilute systems [17], the velocity correlations increase with the density. Although the existence of these correlations restricts the range of validity of the Enskog equation, the latter can be still considered as a good approximation especially at the level of macroscopic properties (such as transport coefficients). In particular, the Enskog results are in quite good agreement with MD simulations and even with real experiments. In the case of computer simulations, comparison between the Enskog theory and MD simulations in the case of the self-diffusion coefficient [18] and kinetic temperatures in a granular mixture [19] have shown good agreement for all α at $n^* \equiv n\sigma^3 \lesssim 0.25$ and up to high densities at $\alpha \gtrsim 0.9$. Here, n is the number density and σ is the diameter of spheres. A theory for densities above the crystallization threshold is not available to our knowledge. The Enskog transport coefficients [8] have also been tested against real NMR experiments of a system of mustard seeds vibrated vertically [20]. The averaged value of the coefficient of restitution of the grains used in this experiment is $\alpha = 0.87$, which lies outside of the quasielastic limit ($\alpha \approx 0.99$). Comparison between theory and experiments shows that the Enskog kinetic theory [8] successfully models the density and granular temperature profiles away from the vibrating container bottom and quantitatively explains the temperature inversion observed in experiments. All these results clearly show the applicability of the Enskog theory for densities outside the Boltzmann limit ($n^* \to 0$) and values of dissipation beyond the quasielastic limit.

Most of the comparisons carried out between kinetic theory results, MD and especially hard sphere event-driven (ED) simulations have been devoted to monodisperse systems, where all the grains have the same mass and size. Needless to say, a real granular system is usually characterized by some degrees of polydispersity in mass and size, which can lead to segregation in an otherwise homogeneous mixture. Almost no research is available for poly-disperse systems but – like in the present study – the bi-disperse systems are frequently examined. As kinetic theory predicts for the homogeneous state [16,22–24], MD simulations [19,27] show that the kinetic temperatures for each species are clearly different and present a complex dependence on the parameters of the problem (dissipation, mass ratio, size ratio, composition, and density). In the case of shearing flow states, recent MD simulations have been performed [28,29] to analyze the (bulk) rheological properties of granular mixtures under uniform shear flow (USF) conditions. Numerical results for the shear stress and the granular energy were compared with those derived from a kinetic theory valid in the low dissipation limit [30, 31]. The comparison between theory and simulation shows an excellent agreement in the quasielastic limit even at large size disparities. Given that this theory [30,31] only applies for weak inelasticity, it assumes energy equipartition and the granular temperature coincides with the partial temperatures of each species. However, beyond the low-dissipation limit, the failure of energy equipartition in granular fluids has not only been predicted by numerical "experiments" [15,16,19, 24–27] but also was observed in real experiments [32,33].

In spite of the agreement found between Enskog kinetic theory and MD simulations and real experiments, there are some reservations in granular fluids community about the usefulness of the Enskog equation to predict macroscopic properties (e.g, transport coefficients) beyond the quasielastic limit. In this context, it would be desirable to perform quite careful comparisons between theory and simulation to establish the limits of validity of the Enskog approximation. This is the primary motivation of this paper. On the other hand, in order to give some insight into this general problem, this hotly current topic can be resolved in a clearer way by considering idealized conditions which are complementary to more phenomenological descriptions of more realistic driven flows. Specifically, our goal here is to make a exhaustive comparison between the Enskog and MD results for two- and three-dimensional granular mixtures under USF. This is a well-known nonequilibrium problem widely studied, for both granular [35–43] and conventional [44] gases. The USF state is perhaps the simplest flow problem since the only nonzero gradient is $\partial u_x/\partial y = a \equiv$ const., where $\mathbf{u}$ is the flow velocity and a is the constant shear rate. Due to its simplicity (as a matter of fact, it becomes *homogeneous* in the Lagrangian frame moving with the flow velocity $\mathbf{u}$ and so boundary effects are avoided in the problem), this state can be used as a prototype problem to shed light on the complexities associated with the behavior of the system under extreme conditions (strong shearing). For this reason, although the state considered here is quite idealized from an experimental point of view, we chose it to determine in a efficient way the dependence of rheology on dissipation. Given that MD simulation avoids any assumption inherent in the Enskog equation, the comparison between kinetic theory and simulation allows us to assess the range of applicability of the Enskog approximation for a quite idealized system but also complicated at the same time. Since the parameter space over which the Enskog equation is verified is quite large (mass ratio, size ratio, mole fraction, density and three independent coefficients of restitution), the test of the kinetic theory is quite stringent. The comparison carried out here shows that the dependence of the rheological properties on mechanical properties and state conditions obtained from the Enskog kinetic theory presents good agreement with MD simulations, except at high density and strong dissipation. In addition, the agreement between kinetic theory and simulation results is better than the one previously reported for the homogeneous cooling state [19], where no energy is fed into the system. Therefore, our results

show again that the Enskog equation is still a valuable tool for granular media since it provides a unique basis for the description of dynamics across a wide range of densities, length scales, and degrees of dissipation. One observation is that no other theory for finite density systems with such generality exists.

It must be noted that our analysis is restricted to the *uniform* shear flow without paying attention to the possible formation of particle clusters (microstructure). Both kinetic theory and DSMC results intrinsically assume homogeneity, whereas in MD fluctuations are intrinsic, and even some degrees of inhomogeneity in density, temperature or shear rate can evolve in a steady state [45]. This can be a possible source of discrepancies between the Enskog results and MD simulations. However, in the USF problem due to the viscous heating, inhomogeneities are weaker than for free cooling systems where clusters continuously grow in size until they reach system size. In addition, given that this instability is confined to long wavelengths, it can be avoided for small enough systems. Here, we have restricted ourselves to rather small systems and so, there was no significant clustering in our MD simulations. For a more detailed study of inhomogeneities in dense binary mixtures involving also collision probabilities and structures, see Ref. [45].

The plan of this paper is as follows. In section 2 we review the Enskog kinetic theory for USF in the case of inelastic systems along with brief descriptions of the Monte Carlo and molecular dynamics simulation methods for the USF. The comparison between the Enskog results and MD simulations is made in section 3 for two- and three-dimensional granular mixtures. We close the paper in section 4 with a discussion of the results presented in this paper.

2 Enskog kinetic theory and simulation methods

We consider a binary mixture of $N = N_1 + N_2$ smooth hard spheres ($d = 3$) or disks ($d = 2$) of diameters σ_1 and σ_2, and masses m_1 and m_2. The collisions between particles of different species are characterized by three independent (constant) coefficients of normal restitution α_{11}, α_{22}, and $\alpha_{12} = \alpha_{21}$, with values $0 < \alpha_{ij} \leq 1$, where α_{ij} refers to collisions between particles of species i and j. The unit vector directed along the line of centers from the particle of species i to the particle of species j upon collision (i.e. at contact) is $\widehat{\boldsymbol{\sigma}}$. The relative velocity of the two particles is $\mathbf{g} = \mathbf{V}_1 - \mathbf{V}_2$, and primes on the velocities denote the initial values $\{\mathbf{V}_1', \mathbf{V}_2'\}$ that lead to unprimed velocities after a binary collision:

$$\mathbf{V}_1' = \mathbf{V}_1 - \mu_{ji}\left(1+\alpha_{ij}^{-1}\right)(\widehat{\boldsymbol{\sigma}}\cdot\mathbf{g})\widehat{\boldsymbol{\sigma}},$$
$$\mathbf{V}_2' = \mathbf{V}_2 + \mu_{ij}\left(1+\alpha_{ij}^{-1}\right)(\widehat{\boldsymbol{\sigma}}\cdot\mathbf{g})\widehat{\boldsymbol{\sigma}}, \quad (1)$$

with $\mu_{ij} = m_i/\left(m_i + m_j\right)$. For later use in kinetic theory integrals, the velocities before collision are expressed as functions of the velocities after collision in equation (1), implicitly defining the (inverse) restitution coefficients used below in equation (6).

2.1 Uniform shear flow

Let us assume that the mixture is under USF conditions. In this state the gas can be enclosed between two infinite parallel plates located at $y = -L/2$ and $y = +L/2$, respectively, and in relative motion with velocities $-U/2$ and $+U/2$, respectively, along the (shear) x-direction. The x-y plane is referred to as the shear-plane in the following. Since an infinite system cannot be realized in a numerical simulation, periodic boundaries are imposed in the (shear) x-direction, and in the third, z-direction perpendicular to the shear plane (for three dimensional situations). The volume of the system is thus the product of the lengths of the periodic box, $V = LX$ (2D) and $V = LXZ$ (3D), with the side lenghts X, L, and Z, of the periodic box, in x-, y-, and z-direction, respectively.

In order to avoid unwanted boundary effects, the walls are replaced by virtual x-z-planes. Also particles crossing such a plane are subjected to (special) periodic boundary conditions. In order to achieve the USF state, Lees–Edwards boundary conditions [46,47] are applied. Here the planes do not represent realistic bounding walls, in contrast to what happens in the true Couette flow [48]. Instead, the planes represent periodic boundary conditions in the local Lagrangian frame moving with the flow velocity of the gas. The periodic images of the system in positive and negative y-direction are moving with velocities $+U/2$ and $-U/2$, respectively.

Under these conditions, the fluid undergoes simple shear with the local velocity field given by

$$\mathbf{u} = ay\widehat{\mathbf{x}}, \quad a = \frac{\partial u_x}{\partial y} = \text{const.}, \quad (2)$$

where a is the (constant) shear rate or velocity gradient and $\mathbf{u}$ refers to the (common) flow velocity. In addition, the partial densities of each species $n_i = N_i/V$ and the granular temperature T (defined below) are uniform, while the mass and heat fluxes vanish for symmetry reasons. For higher densities and stronger dissipation as used in our paper, a, n_i and T can become functions of the position so that the USF assumptions are not valid anymore [63].

The only relevant macroscopic balance equation in the USF problem corresponds to the balance equation for the temperature T. It is given by [49]

$$\frac{\partial}{\partial t}T = -\frac{2}{dn}aP_{xy} - \zeta T, \quad (3)$$

where $n = n_1 + n_2$ is the total number density, P_{xy} denotes the xy element of the total pressure tensor of the mixture, and ζ is the cooling rate due to collisions among all the species. According to equation (3), the temperature changes in time due to the competition between two mechanisms: on the one hand, viscous (shear) heating and, on the other hand, energy dissipation in collisions. In the steady state, both mechanisms cancel each other and the (steady) temperature is obtained by equating the production term due to shear work with collisional dissipation:

$$aP_{xy} = -\frac{d}{2}nT\zeta. \quad (4)$$

This steady shear flow state is what we want to analyze here.

The balance equation (4) shows the intrinsic connection between the shear field and dissipation in the system. This is a peculiar feature of granular fluids since there is an internal mechanism for which the collisional cooling sets the strength of the velocity gradient. This contrasts with the description of USF for elastic fluids where a steady state is not possible unless an external thermostat is introduced [44]. Therefore, for given values of the parameters of the mixture, in the steady state the reduced shear rate (which is the relevant nonequilibrium parameter of the problem) $a^* \propto a/\sqrt{T}$ is a function of the coefficients of restitution α_{ij} only [50]. In particular, the *quasielastic* limit ($\alpha \to 1$) naturally implies the limit of *small* shear rates ($a^* \ll 1$) and vice versa. Since the limit of small shear rates also implies a continuum-level description of the Enskog kinetic equation at the Navier–Stokes order, we may conclude that in the USF the full nonlinear dependence of the shear viscosity on the shear rate cannot be obtained from the Navier-Stokes approximation, at least for finite dissipation [50]. We shall come back to this point while discussing our results.

2.2 Enskog kinetic theory

As said above, at a microscopic level the USF is generated by Lees–Edwards boundary conditions [46,47] which are periodic boundary conditions in the local Lagrangian frame $\mathbf{V} = \mathbf{v} - \mathsf{a}\cdot\mathbf{r}$ and $\mathbf{R} = \mathbf{r} - \mathsf{a}\cdot\mathbf{r}t$. Here, a is the tensor with elements $a_{k\ell} = a\delta_{kx}\delta_{\ell y}$. In terms of the above variables, the one-particle velocity distribution functions $f_i(\mathbf{V})$ ($i = 1, 2$) are uniform [51] and the Enskog equation takes the form

$$aV_y \frac{\partial}{\partial V_x} f_i = \sum_{j=1}^{2} J_{ij}^{\mathrm{E}}\left[\mathbf{V}|f_i, f_j\right], \tag{5}$$

where the Enskog collision operator $J_{ij}^{\mathrm{E}}\left[\mathbf{V}|f_i, f_j\right]$ reads [49]

$$\begin{aligned} J_{ij}^{\mathrm{E}}\left[\mathbf{V}_1|f_i, f_j\right] = \sigma_{ij}^{d-1}\chi_{ij}\int d\mathbf{V}_2 \int d\widehat{\boldsymbol{\sigma}}\,\Theta(\widehat{\boldsymbol{\sigma}}\cdot\mathbf{g})(\widehat{\boldsymbol{\sigma}}\cdot\mathbf{g}) \\ \times\left[\alpha_{ij}^{-2} f_i(\mathbf{V}_1')f_j(\mathbf{V}_2' + a\sigma_{ij}\widehat{\sigma}_y\widehat{\mathbf{x}}) \right. \\ \left. - f_i(\mathbf{V}_1)f_j(\mathbf{V}_2 - a\sigma_{ij}\widehat{\sigma}_y\widehat{\mathbf{x}})\right]. \end{aligned} \tag{6}$$

Here, $\boldsymbol{\sigma}_{ij} = \sigma_{ij}\widehat{\boldsymbol{\sigma}}$ with $\sigma_{ij} = \left(\sigma_i + \sigma_j\right)/2$, Θ is the Heaviside step function and the velocities were defined before in equation (1). In addition, we have taken into account that the pair correlation function χ_{ij} is uniform in the USF problem.

The rheological properties of the system are quantified by the pressure tensor $\mathbf{P}$, which is the only relevant flux in the USF problem. The expression for the pressure tensor $\mathbf{P}$ contains both *kinetic* and *collisional* transfer contributions. Their explicit forms for the USF problem can be found in Ref. [49]. Apart from getting the elements of the pressure tensor, it is also interesting to determine the temperature ratio T_1/T_2 where the partial temperatures T_i are defined as

$$T_i = \frac{m_i}{dn_i}\int d\mathbf{V}\, V^2 f_i(\mathbf{V}). \tag{7}$$

In terms of the partial temperatures, the granular temperature T is defined as

$$T = x_1 T_1 + x_2 T_2, \tag{8}$$

where $x_i = n_1/n$ is the mole fraction of species i. As we will show later, the equipartition of energy is broken in a granular mixture, so that the kinetic temperatures T_i of each species differ from the (global) temperature T. This is a consequence of the inelasticity of collisions. It must be noted that the fact that $T_1 \neq T_2$ does not mean that there are additional hydrodynamic degrees of freedom, since T_1 and T_2 can be expressed in terms of the granular temperature T, which is the relevant temperature at a macroscopic level. The deviation of T_1/T_2 from unity is a measure of the breakdown of the energy equipartition.

In spite of the simplicity of the USF problem, only two special situations allow for simple analytical results. First, in the low density limit, the corresponding Boltzmann equation can be approximately solved by Grad's method [52]. This solution compares quite well with Monte Carlo simulations [52–54], even for strong dissipation. Second, for small shear rates but finite densities, the Enskog equation can be solved by the Chapman–Enskog method [55] and an explicit expression for the Navier–Stokes shear viscosity coefficient has been obtained in the leading Sonine approximation [49]. It must be remarked that the kinetic theory derived in Ref. [49] differs from the one previously obtained in Ref. [30] since the former should apply for an arbitrary degree of dissipation and takes into account the effect of temperature differences on momentum transport. Beyond the above two special cases (dilute gas and Navier–Stokes approximation), Lutsko [56] has recently solved the Enskog equation for a moderately dense mixture under USF by using a generalized moment method. Although this theory compares quite well with MD simulations, it appears too complicated to be useful for practical purposes here, since it involves many different collision integrals that must be solved numerically. Instead, as an alternative to the above theory [56], we compute here the rheological properties from a *numerical* solution of the Enskog equation by means of an extension of the well-known Direct Simulation Monte Carlo (DSMC) method [57] to dense gases [57–59].

2.3 Enskog simulation Monte Carlo method for USF

As said before, due to the mathematical complexity of the Enskog collision operator, here we will use an extension of the DSMC method to dense gases to numerically solve equation (5). This method is usually referred to as the Enskog Simulation Monte Carlo (ESMC) method. This procedure was devised to mimic the dynamics involved in the Enskog collision term (still assuming operator-splitting and molecular chaos), and it has been compared to hard sphere simulations in vibrated and freely cooling systems [9–11,59] and more previously has been used to analyze rheological properties of monocomponent systems for both the elastic [58] and the inelastic [24,25,61] case. For a detailed description of the method applied to inelastic systems, we refer the reader to Refs. [24,25] and [49].

From the simulations, one evaluates the kinetic $\mathbf{P}^{\mathrm{k}}$ and collisional $\mathbf{P}^{\mathrm{c}}$ contributions to the pressure tensor:

$$\mathbf{P}^{\mathrm{k}} = \sum_{i=1}^{2} \frac{m_i n_i}{N_i} \sum_{k=1}^{N_i} \mathbf{V}_k \mathbf{V}_k, \tag{9}$$

and

$$\mathbf{P}^{\mathrm{c}} = \frac{n}{2N\Delta t} \sum_{k\ell}^{\dagger} \frac{m_i m_j}{m_i + m_j} \sigma_{ij} (1+\alpha_{ij}) (\mathbf{g}_{k\ell} \cdot \widehat{\boldsymbol{\sigma}}_{k\ell}) \widehat{\boldsymbol{\sigma}}_{k\ell} \widehat{\boldsymbol{\sigma}}_{k\ell}. \tag{10}$$

The partial temperatures T_i are given by

$$T_i = \frac{m_i}{d N_i} \sum_{k=1}^{N_i} V_k^2. \tag{11}$$

In the above equations, N_i is the number of "simulated" particles of species i, $N = N_1 + N_2$ is the total number, Δt is the time step used, and the dagger (†) means that the summation is restricted to the accepted collisions [24,25,49]. In addition, k denotes a particle of species $i = 1, 2$ and ℓ a particle of species $j = 1, 2$, so that all possible types of collisions between species are accounted for. To improve the statistics, the results are averaged over a number $\mathcal{N}$ of independent realizations or replicas. In our simulations we have typically taken a total number of particles $N = 10^5$, a number of replicas $\mathcal{N} = 10$, and a time step $\Delta t = 3 \times 10^{-3} \lambda_{11} / V_{01}(0)$. Here, $\lambda_{11} = (\sqrt{2} n_1 \widetilde{\sigma}_{11})^{-1}$ is the mean free path for collisions of species 1–1 and $V_{01}^2(0) = 2T(0)/m_1$, where $T(0)$ is the initial temperature. Here, $\widetilde{\sigma}_{ij}$ means the total cross-section for collisions of species i–j [For hard disks, $\tilde{\sigma}_{ij} = \sigma_{ij}$ while $\tilde{\sigma}_{ij} = \pi \sigma_{ij}^2$ for hard spheres]. More technical details on the application of the ESMC method to USF can be found in Ref. [49].

In the simulations the initial velocity distribution function is that of local equilibrium, i.e. a Gaussian. The ESMC simulation is prepared as follows: after an initial transient period, the system reaches a steady state where the values obtained for the reduced quantities, see below equations (13)–(15), are independent of the initial preparation of the system. Their values do depend on the values of the coefficients of restitution, the packing fraction, and the ratios of mass, concentrations and sizes.

2.4 Event-driven simulation method for uniform shear flow

The MD and ED simulation methods are extensively discussed, e.g. in textbooks [47], for elastic systems, and were also applied to sheared granular systems, see Refs. [29,62,63] and references therein. In event-driven simulations, we drive a collection of smooth inelastic particles (disks in 2D and spheres in 3D) in a square/cubic box of size $X = Z = L$ by uniform shear flow, using the Lees–Edwards boundary conditions [46,47], as introduced at the beginning of this section. The particles are initially placed randomly in the computational box, and the initial velocity field is composed of the uniform shear and a small Gaussian random part.

Since the particles are perfectly rigid (i.e. the hard-core potential), the collisions are instantaneous and the simulation moves in time from one collision to the next. The pre- and post-collisional velocities of two colliding particles are related by equation (1). The expression for the collisional impulse is

$$\mathbf{I}_{ij} \equiv m_i (\mathbf{V}_i - \mathbf{V}_i') = \frac{m_i m_j}{m_i + m_j} (1+\alpha_{ij}) (\widehat{\boldsymbol{\sigma}} \cdot \mathbf{g}) \widehat{\boldsymbol{\sigma}}, \tag{12}$$

which is used to calculate the collisional contributions to the transport coefficients [29]. In steady state, the uniform shear flow attains a constant granular energy owing to the balance between the shear work and the collisional dissipation. After reaching this steady state, the simulation was allowed to run for at least another 4, 000 collisions per particle to gather data to calculate the rheological quantities.

Along with the granular energy, we have also monitored the linearity of the streamwise velocity profile across the shear gap between $y = -L/2$ and $y = L/2$. We have found that the calculated shear rate (i.e. the slope of the velocity profile) fluctuated around the imposed shear rate by less than 1% for all cases studied here. Another important issue in ED simulations is that the sheared granular systems are prone to the clustering instability. However, only for large systems with strong dissipation ($\alpha \leq 0.8$), the clusters become visible, and the cluster-size increases with increasing dissipation and mass-disparity [45]. In an effort to eliminate/minimize the clustering instability, we have restricted ourselves to rather small systems, i.e. $N \leq 1,000$.

2.5 Rheology

The rheological properties of the mixture are determined from the nonzero elements of the pressure tensor. Possibilities to non-dimensionalize are to scale either by the relevant large species contributions [29] or by the corresponding mean values [63]. Applying the former scheme, one arrives at the reduced shear viscosity

$$\mu = \frac{|P_{xy}|}{\varrho_1 \sigma_1^2 a^2}, \tag{13}$$

the reduced temperature

$$\theta = \frac{T}{m_1 \sigma_1^2 a^2}, \tag{14}$$

and the reduced pressure

$$\Pi = \frac{p}{\varrho_1 \sigma_1^2 a^2}, \quad p = \frac{1}{d} \mathrm{tr}\, \mathbf{P}. \tag{15}$$

Here, $\mathrm{tr}\, \mathbf{P}$ denotes the trace of the pressure tensor $\mathbf{P}$ and ϱ_i is the material density of species i. In the case of hard disks $\varrho_i = 4m_i/\pi\sigma_i^2$ while $\varrho_i = 6m_i/\pi\sigma_i^3$ for hard spheres.

As said before, in the steady state and for given values of the parameters of the mixture, the (dimensionless) rheological properties μ, θ, and Π are functions of the coefficients of restitution α_{ij} only, and their dependencies on the shear rate

are scaled out. The parameters of the mixture are the mass ratio m_1/m_2, the mole fraction $x_1 = n_1/n$, the ratio of diameters σ_1/σ_2, and the total solid volume fraction $\phi = \phi_1 + \phi_2$ where $\phi_i = n_i m_i/\varrho_i$ is the species volume fraction of component i.

3 Results

The main objective of this Section is to compare the results on the pressure, shear viscosity and granular temperature obtained from the ESMC method with those obtained from MD simulations performed for bidisperse mixtures of smooth hard disks ($d = 2$) and hard-spheres ($d = 3$). In addition, we also present results for the temperature ratio and normal stress differences. For the sake of simplicity, we assume that all the coefficients of restitution are set equal ($\alpha_{ij} \equiv \alpha$) so that the parameter space of the problem is reduced to five quantities: $\{\alpha, \phi, m_1/m_2, \sigma_1/\sigma_2, x_1\}$, where $m_1 \geq m_2$ and $\sigma_1 \geq \sigma_2$ is implied in the following. Three different values of the solid volume fraction ϕ have been considered here, $\phi = 0.05$, $\phi = 0.1$, and $\phi = 0.2$. The first value of ϕ represents a dilute gas while the two latter can be considered as moderately dense fluids. In the following, an equimolar mixture ($x_1 = 1/2$) with particles of equal size ($\sigma_1 = \sigma_2$) but with different masses is examined. More specifically, we have studied the dependence of μ, θ, Π, and the temperature ratio T_1/T_2 on the mass ratio m_1/m_2 for different values of α and ϕ in both two and three dimensions.

3.1 2D results

For the pair correlation function values at contact in 2D, χ_{ij}, the relation [65]

$$\chi_{ij} = \frac{1}{1-\phi} + \frac{9}{16}\frac{\beta}{(1-\phi)^2}\frac{\sigma_i\sigma_j}{\sigma_{ij}}, \tag{16}$$

is used in the Enskog and ESMC calculations, where $\beta = \pi(n_1\sigma_1 + n_2\sigma_2)/4$. The approximation (16) for the equilibrium pair correlation function is accurate in most of the fluid region, although a more detailed comparison with computer simulations shows that the expression becomes less accurate with increasing density and diameter ratios [65]. However, given the values considered in our simulations, we expect that these approximations to χ_{ij} turn out to be reliable with an error margin of much less than one per-cent, so that we do not consider the higher order corrections here.

In Figures 1 and 2, we plot Π, μ, θ, and T_1/T_2 against m_1/m_2 for a low density, $\phi = 0.05$, and the coefficients of restitution $\alpha = 0.9$ and $\alpha = 0.75$, respectively. The symbols refer to MD simulations (triangles) and ESMC results (circles) while the solid lines correspond to the analytical results obtained by solving the Boltzmann equation [52,54] (which is strictly valid in the limit $\phi \to 0$) by means of Grad's moment method. In Figure 1, the agreement between the ESMC and MD results is excellent, even for very disparate masses. The Boltzmann results compare also quite well with simulations, especially in the case of low temperature ratios.

For the steady temperature, the Boltzmann predictions slightly overestimate the MD simulation results. These discrepancies can be primarily attributed to density effects, since previous comparisons between theory and DSMC results show better agreement for $\phi = 0$ than the one reported here [54]. Comparing the two figures, one can conclude that the agreement between the Boltzmann kinetic theory and the simulation data becomes worse with increasing dissipation. The only exception is the temperature ratio which is essentially obtained from the diagonal elements of the kinetic contribution to the pressure tensor. We also observe good agreement between ESMC and MD results, except for the largest values of the mass ratio considered.

Both Enskog (ESMC) and MD results clearly predict a *non-monotonic* behavior of the pressure and the viscosity with the mass ratio. This observation contrasts with the predictions of kinetic theories [30,31] based on the equipartition assumption which suggest a monotonic dependence of Π and μ on m_1/m_2 [38,48]. With respect to the behavior of the temperature ratio, we observe that T_1/T_2 strongly increases with the mass ratio. The mass disparity enhances the magnitude of the non-equipartition of energy [29].

Figures 3 and 4 depict results for the higher densities $\phi = 0.1$ and $\phi = 0.2$, with a coefficient of restitution $\alpha = 0.9$. As in the case of dilute mixtures (Figures 1 and 2), the Enskog (ESMC) results agree well with the MD simulations, only does the discrepancy increase in general with decreasing mass ratio for the pressure Π and the temperature θ, while the opposite occurs for the temperature ratio. We also observe that in general the Enskog kinetic theory underestimates the MD results. For instance, in the case $m_1/m_2 = 4$ and for $\phi = 0.2$, the discrepancies for Π, μ, T_1/T_2, and θ are about 5, 7, 7, and 5%, respectively. In addition, both Enskog and MD results clearly predict a *non-monotonic* behavior of the pressure and the viscosity on the mass ratio. This conclusion contrasts with the predictions of kinetic theories [30, 31] based on the equipartition assumption which suggest a monotonic dependence of Π and μ on m_1/m_2 [54,63]. Also for higher densities, T_1/T_2 increases strongly with the mass ratio. Differences between the Enskog theory and MD simulations become more significant as the dissipation increases, as shown in Figure 5 for $\phi = 0.2$ and $\alpha = 0.75$. Although the Enskog theory captures well the trends observed in MD simulations, the disagreement between both approaches is more important than the one observed in previous cases. More specifically, in the case $m_1/m_2 = 4$, the discrepancies for Π, μ, T_1/T_2, and θ are now about 9, 6, 11, and 10%, respectively. However, given that these deviations are not quite large, one can still consider the Enskog equation as a good approximation for describing the rheological properties of a granular mixture, even for moderately high density and strong dissipation.

Before discussing the possible reasons for the discrepancy, the three-dimensional results are presented in the following sub-section.

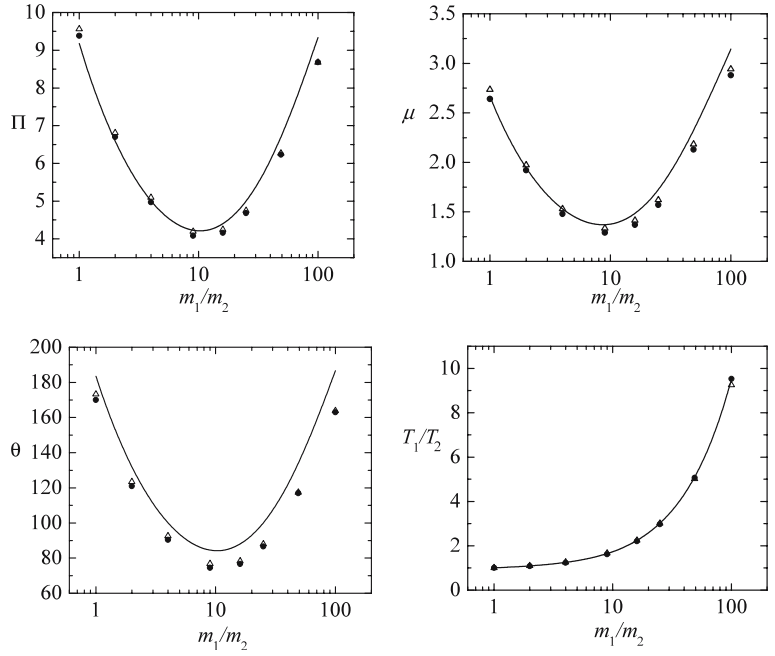

Fig. 1 Reduced pressure Π, reduced shear viscosity μ, reduced temperature θ and temperature ratio T_1/T_2 plotted against the mass ratio m_1/m_2 for an equimolar mixture ($x_1 = 1/2$) of hard disks ($d = 2$) with $\sigma_1/\sigma_2 = 1$, $\phi = 0.05$ and $\alpha = 0.9$. The lines are the analytical results obtained from the Boltzmann kinetic equation while the symbols correspond to the ESMC results (*solid circles*) and MD simulations (*open triangles*)

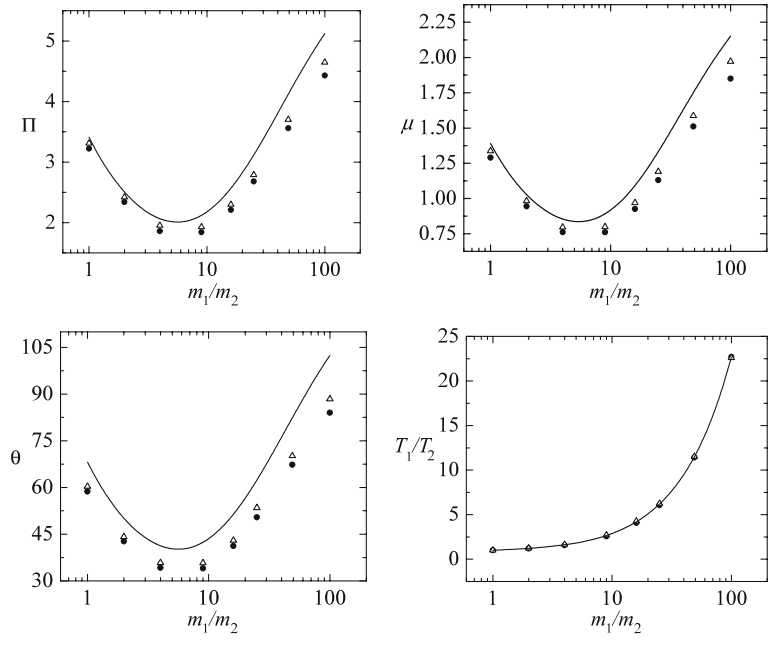

Fig. 2 The same as Figure 1, only with $\alpha = 0.75$. Note the different axis scaling as compared to Figure 1

3.2 3D results

In the case of hard spheres ($d = 3$), we take for the pair correlation function χ_{ij} the following approximation [66,67]

$$\chi_{ij} = \frac{1}{1-\phi} + \frac{3}{2}\frac{\beta}{(1-\phi)^2}\frac{\sigma_i\sigma_j}{\sigma_{ij}} + \frac{1}{2}\frac{\beta^2}{(1-\phi)^3}\left(\frac{\sigma_i\sigma_j}{\sigma_{ij}}\right)^2, \tag{17}$$

where now $\beta = \pi(n_1\sigma_1^2 + n_2\sigma_2^2)/6$. We compare the ESMC and MD results obtained for a mixture under USF with a kinetic theory recently proposed [49]. In contrast to previous theories [30], the above theory takes into account the effect of non-equipartition of granular energy on the transport coefficients. This theory is based on the Chapman–Enskog solution [55] to the Enskog equation in the first order of the shear rate (Navier–Stokes-level approximation). However, given that USF is inherently non-Newtonian, the full

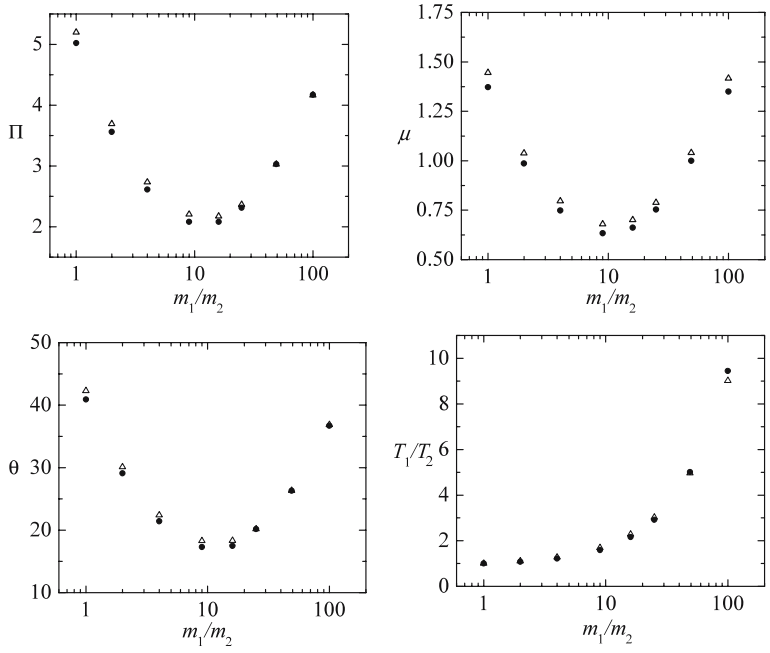

Fig. 3 The same as Figure 1, only with $\phi = 0.1$

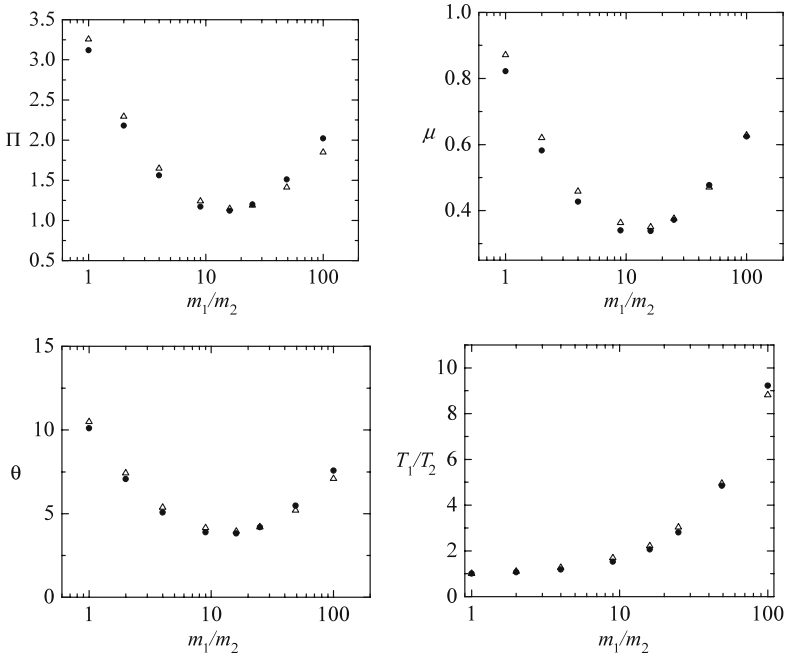

Fig. 4 The same as Figure 1, only with $\phi = 0.2$

nonlinear dependence of the viscosity on the shear rate is required. This implies that there is no possibility a priori of using the Navier–Stokes equations to describe the (shear-rate dependent) rheological properties of USF, especially as the dissipation increases [50].

Figure 6 shows the variations of pressure (Π), shear viscosity (μ), granular temperature (T) and the temperature ratio (T_1/T_2) with the mass ratio for the volume fraction $\phi = 0.1$. The coefficient of restitution is set to 0.9, and the other parameters are $\sigma_1/\sigma_2 = 1$ and $x_1 = 1/2$. The solid lines represent the Chapman–Enskog solution to the Enskog equation [49], and the symbols represent the MD simulation results. It must be stressed that we have also considered other systems with different densities, finding similar results as before for the two-dimensional situation. Therefore, we do not show more 3D results here for the sake of brevity. We observe that, as in the 2D case, the pressure, the viscosity and the granular temperature vary non-monotonically with the

mass-ratio. Comparing our results for 3D and 2D, we find that for any given density the magnitudes of the scaled quantities Π, μ, and T are much lower in 3D; however, the temperature ratio (T_1/T_2) remains relatively insensitive to the dimension. Concerning the comparison between ED simulations and the Chapman–Enskog solution, we observe that although the latter captures well the main qualitative trends observed for the rheological properties in the simulation, there are significant quantitative discrepancies between both descriptions.

To assess the influence of dissipation on rheology, the reduced quantities Π, μ, θ, and T_1/T_2 are plotted in Figure 7 as a function of the coefficient of restitution α for $\sigma_1/\sigma_2 = 1$, $x_1 = 1/2$, $m_1/m_2 = 4$, and $\phi = 0.1$ as given by ESMC (circles) and MD simulations (triangles) and the Chapman-Enskog solution (solid lines). Given that in reduced units, the shear rate and dissipation are not independent parameters, one would expect that the differences between the Navier-Stokes-level predictions and the simulation results increase as the coefficient of restitution decreases. Figure 7 confirms this since, for instance, the discrepancies between theory and MD simulations for Π, μ, θ, and T_1/T_2 are about 30, 43, 32, and 10%, respectively, for $\alpha = 0.7$. Such large discrepancies between theory and simulation can be tied to the non-Newtonian behaviour of the USF state [50,62], as we show below, in the next figure. Concerning the comparison between the ESMC and MD results, we observe good agreement as in the 2D case, except for strong dissipation where the discrepancies are important (say, for instance, about 10% for $\alpha = 0.7$).

One possible reason for the discrepancy between Enskog and MD results is the enhanced correlations in a sheared granular mixture with increasing dissipation [45]. In particular, it has been shown [45,62] that the probability of particle collisions on their upstream faces increases with increasing dissipation, leading to enhanced positional and velocity correlations. Such correlated collisions are, by construction, not taken into account in the Enskog theory.

Another source of dicrepancy between the Chapman–Enskog solution and simulations is the inherently non-Newtonian nature of flow, i.e. the granular fluid supports large normal stress differences [34,50,62]. A quantitative measure of the stress differences are the first ψ_1 and the second ψ_2 viscometric functions. They are defined as

$$\psi_1 = \frac{P_{xx} - P_{yy}}{p}, \quad \psi_2 = \frac{P_{yy} - P_{zz}}{p}. \tag{18}$$

Note that we have scaled both these viscometric functions by the pressure to ascertain their relative magnitude with respect to it [29,62]. Of course, non-zero values of ψ_1 and ψ_2 would indicate that the granular fluid is non-Newtonian. Figure 8 shows the variations of the first (ψ_1) and second (ψ_2) normal stress differences with the coefficient of restitution α for an inelastic hard-sphere (3D) mixture: $x_1 = 1/2$ $\phi = 0.1$, $\sigma_1/\sigma_2 = 1$ and $m_1/m_2 = 4$. Since the Chapman–Enskog solution gives $\psi_1 = \psi_2 = 0$, here we have only compared the ESMC and ED results. For the systems considered, we observe that ψ_1 is positive but ψ_2 is negative, and both increase in magnitude with increasing strength of dissipation. In general, ψ_2 is typically an order of magnitude smaller than ψ_1. Note that at much higher density as considered here, ψ_1 will become also negative near the freezing density, and ψ_2 becomes positive at $\phi \approx 0.15$ [62]. These overall features are similar to those of the monodisperse sheared granular fluid [62].

For a monodisperse sheared granular fluid, it has been shown [29] that one reason for the discrepancy between the simulation results and the Navier–Stokes level theory is that the latter does not take into account anisotropies in the second moment of velocity fluctuations that gives rise to the "measurable" normal stress differences. However, this requires a Burnett-order constitutive theory [34,35,50]. Once we incorporate such Burnett-order corrections, the theoretical predictions for the pressure, viscosity and granular temperature agree excellently even at a coefficient of restitution of $\alpha = 0.5$ (see Figure 2 in Ref. [29]). Since the magnitudes of normal stress differences are enhanced in a binary mixture, one expects that the agreement between theory and simulation also improves when Burnett-order corrections to the rheological properties are taken into account.

4 Summary and Discussion

In an effort to validate the Enskog kinetic theory, the Enskog equation for a binary mixture of smooth *inelastic* hard disks/spheres under steady USF has been studied theoretically, by means of ED simulations, and was numerically solved by means of the ESMC method. Results for the (reduced) rheological properties and the temperature ratio have been reported in a wide parameter space (mass ratio, density, and coefficients of restitution). Variations of the diameter ratio and the composition were studied elsewhere [29]. We have chosen this idealized state for a quite complex system to show in a clearer way the dependence of the rheological properties on dissipation in far from equilibrium conditions. This allows us to perform a careful and exhaustive comparison between kinetic theory and ED simulations in order to determine the range of validity of the Enskog approximation. As said in the Introduction, there are some concerns in the granular flow community about the importance of this equation to describe granular flows beyond the quasielastic limit. To clarify this controversy, the results reported here can be used to support the Enskog theory as a valuable tool for qualitatively describing granular flows in an extremely wide parameter space. Since the theory is rather involved, only the comparison with various numerical method will allow for a systematic, step by step improvement and possibly future simplifications in the spirit of applicability. Showing all this has been the main motivation of our work, as well as providing a collection of reference data for other simulation methods, solution techniques and theories.

We have basically focused on studying the combined effect of mass disparity and dissipation on the rheological properties of sheared 2D and 3D granular mixtures. Three different values for the solid volume fraction (ϕ=0.05, 0.1, and 0.2) and two values of the coefficient of restitution (α=0.9

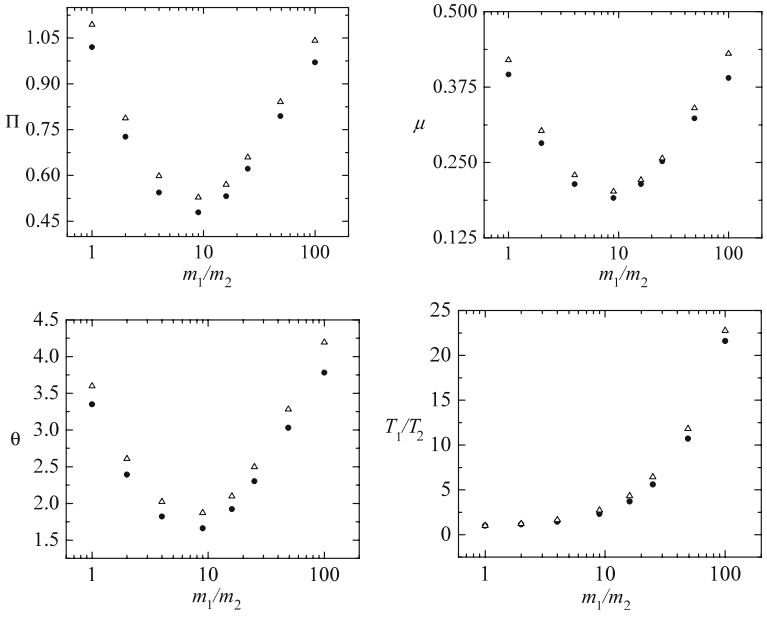

Fig. 5 The same as Figure 1, only with $\phi = 0.2$ and $\alpha = 0.75$

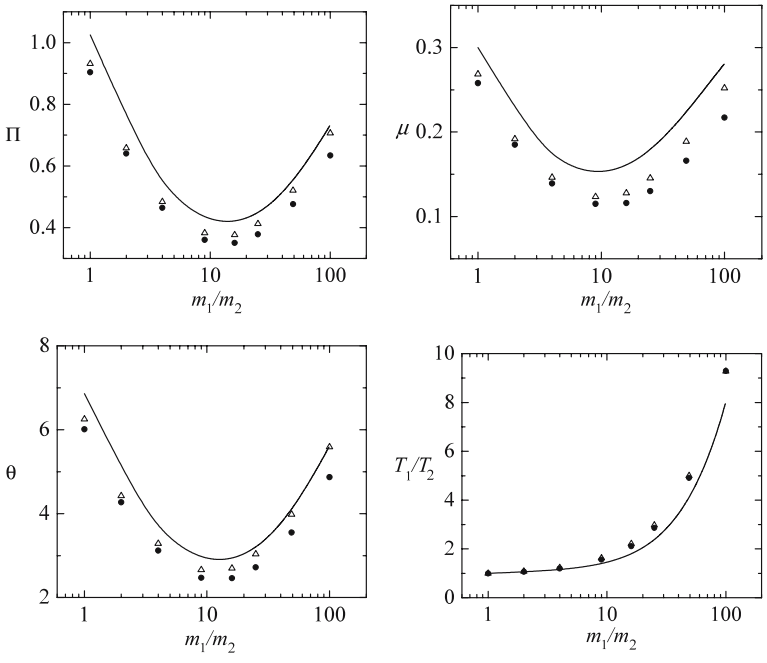

Fig. 6 Same as Figure 1, but at $\phi = 0.1$ and for hard spheres ($d = 3$). The lines are the analytical results obtained from the Chapman–Enskog solution up to the Navier–Stokes order while the symbols correspond to the ESMC results (*solid circles*) and MD simulations (*open triangles*)

and 0.75) were considered. In the case of α=0.9, the comparison shows that there are no significant quantitative differences between the results obtained from MD simulations and those that follow from the ESMC method. As the dissipation increases ($\alpha = 0.75$), although the Enskog predictions compare qualitatively well with MD data, the discrepancies between both approaches become more prominent. These discrepancies tend to increase also with increasing density. On the other hand, the good agreement found here includes densities well outside of the Boltzmann limit and values of dissipation that clearly lie outside of what can be considered the quasielastic limit. This test may be taken again as a further testimony to the usefulness of the Enskog equation for fluids with elastic and inelastic collisions, including mixtures.

Like the Boltzmann equation, the Enskog kinetic theory [24,49] assumes the molecular chaos hypothesis and thus the two particle velocity correlations for a pair of particles at contact are neglected. However, as mentioned in the Introduction,

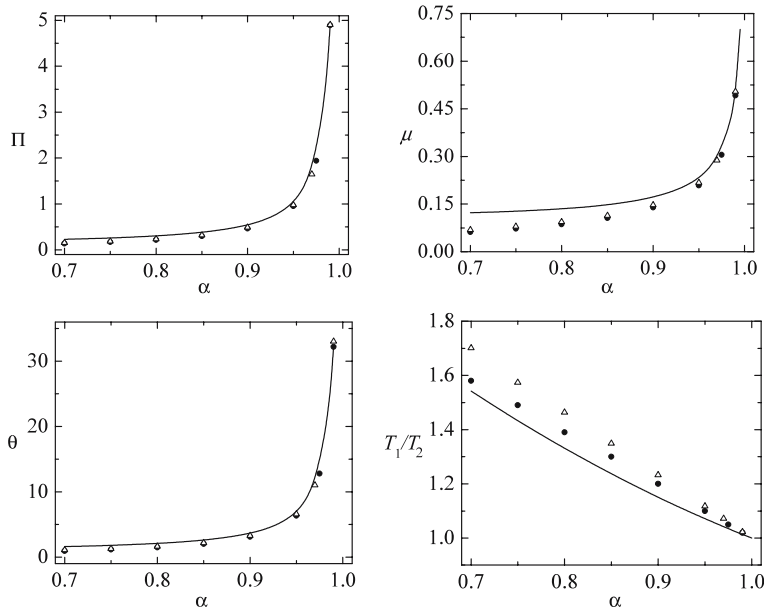

Fig. 7 Plot of the reduced pressure Π, shear viscosity μ, temperature θ and temperature ratio T_1/T_2 versus the coefficient of restitution α for an equimolar mixture ($x_1 = 1/2$) of hard spheres ($d = 3$) with $\sigma_1/\sigma_2 = 1$, $m_1/m_2 = 4$, and $\phi = 0.1$. The lines are the analytical results obtained from the Chapman–Enskog solution up to the Navier–Stokes order while the symbols correspond to the ESMC results (*solid circles*) and MD simulations (*open triangles*)

in recent MD simulations performed in the homogeneous case for driven [12–14] and for undriven [17] granular gases, as well as in sheared granular fluids [45,62], velocity correlations for pairs of particles that are about to collide have been observed. These short-range velocity correlations were relevant for high densities and finite dissipation. Consequently, some disagreement between the Enskog theory and simulations with increasing dissipation is expected. However, given that the magnitude of disagreement with increasing dissipation is not much, one can conclude that the validity of the Enskog kinetic theory appears to span a much wider range than the limit of nearly elastic collisions. On the other hand, the failure of the Enskog kinetic theory at high densities is expected just as for fluids with elastic collisions [68]. This is presumably due to increasingly correlated collisions in a sheared granular fluid in the same limit [62].

There is some indication that the effects of correlated collisions are enhanced by strong dissipation since the colliding particles become more focussed [12–14]. Furthermore, our results also indicate that the range of densities for which the Enskog equation holds decreases with increasing dissipation. This conclusion is in agreement with previous findings made for mixtures in the homogeneous cooling state [19] and for the case of the self-diffusion coefficient [18]. The specific mechanism responsible for the stronger discrepancies at higher densities and its quantitative prediction remains an open issue.

As said in the Introduction, one possible source of discrepancies observed between Enskog (ESMC) results and MD simulations is due to the fact that while the theory and ESMC results are restricted to the homogeneous state (in the Lagrangian frame), some degree of inhomogeneity (especially for density) evolves in MD simulations also in the steady state situation. However, given that this clustering instability is quite significant for large systems and sufficiently strong dissipation, here we have considered small enough systems to avoid this instability as much as possible. Thus, for instance, in all the cases analyzed here the slope of the velocity profile across the shear gap fluctuates around the *imposed* shear rate by at most 1%. On the other hand, in a *driven* (sheared) system, the inhomogeneities are weaker than for a *freely cooling* system where clusters can grow and grow without being disturbed by the action of the energy input. For this reason, the magnitude of the differences between the Enskog predictions and MD simulations observed here are in general smaller than those previously reported in

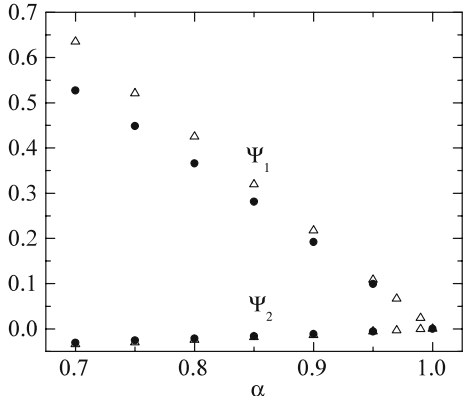

Fig. 8 Variations of the first (ψ_1) and second (ψ_2) normal stress differences with the restitution coefficient for an inelastic hard-sphere (3D) mixture: $x_1 = 1/2$, $\phi = 0.1$, $\sigma_1/\sigma_2 = 1$ and $m_1/m_2 = 4.0$

the undriven homogeneous case [18,19] for the same values of density and coefficient of restitution. Thus the range of densities and dissipation for which the Enskog kinetic theory applies depends not only on dissipation and density but also, rather strongly, on the state of the system and the boundary conditions (means of energy input), and cannot be given as a general rule. For the USF, as considered here, it seems that the Enskog equation can be taken as a reliable model to get the dependence of the rheological properties on the mechanical parameters of the mixture. The qualitative agreement between ESMC and MD is perfect, while small quantitative differences exist.

The (steady) USF problem is inherently non-Newtonian [50,62] since it supports large normal stress differences. Due to the coupling between the reduced shear rate (measured through the reduced temperature θ) and dissipation, large gradients can occur as the system becomes more inelastic. This implies that the shear viscosity coefficient in USF cannot be deduced from the usual Navier–Stokes or Newtonian hydrodynamic equations (which are linear in the gradients) [50]. On the whole, a Burnett-order constitutive theory is a promising approach required for a better agreement between simulations and theory, as shown in the monodisperse case. The comparison carried out in Figure 7 in the case of hard spheres shows that the Navier–Stokes predictions obtained from a recent Chapman–Enskog solution [53] deviate from the ESMC results obtained for USF as the coefficient of restitution decreases (dissipation strength increases). However, the agreement found between theory and ESMC simulations extends beyond the quasielastic limit, (say for instance, for $\alpha \gtrsim 0.97$) except for the temperature ratio. In this spirit, it is possible that the failure of the Navier-Stokes approximation to describe non-Newtonian properties could be in part mitigated by the introduction of appropriate reduced quantities, such as those defined by equations (13)–(15).

Given that the dynamical velocity correlations measured in previous works [12–14] become important as the fluid density increases, some authors [12,17] conclude that the Enskog equation can be insufficient to compute average properties of the fluid. This conclusion contrasts with the results reported in this paper where, at least for the problem studied here, velocity correlations do not seem to play the relevant role and the Enskog equation accurately predicts the rheological properties of the system. In this context, one can conclude that the Enskog equation provides a unique basis for the description of dynamics for a wide range of densities, length scales, and degrees of dissipation. So far, no other theory with such generality exists. However, it is possible that for more complex situations than the one studied here (USF conditions), velocity correlations become important even before the system develops significant spatial correlations and the Enskog theory (which only takes into account spatial correlations) does not provide reliable predictions. In this case, new kinetic theories incorporating the effect of velocity correlations are needed to describe dense granular fluids at finite dissipation.

Starting from the present state, the directions of future research thus are (1) a better understanding of correlations in velocity and positions, (2) a better insight into the non-Newtonian, anisotropic effects, (3) an extension of the bi-disperse methodology towards poly-disperse systems, (4) possibly higher order theories in order to deal with large gradients of, e.g., density, and (5) also to extend present theories towards much higher densities and stronger dissipation.

Acknowledgements Partial support of the Ministerio de Ciencia y Tecnología (Spain) through Grant No. ESP2003-02859 (partially financed by FEDER funds) in the case of J.M.M. and FIS2004-01399 (partially financed by FEDER funds) in the case of V.G. is acknowledged. M.A. and S.L. acknowledge partial supports from the JNCASR (PC/EMU/MA/35) and the AvH Foundation, and S.L. acknowledges partial support from the DFG.

References

1. Ernst, M.H.: In dynamics: models and kinetic methods for non-equilibrium many body systems. In: Karkheck, J. (ed.) Boston: Kluwer Academic, (2000)
2. Pöschel, T., Luding, S.: *Granular gases*. (ed.) Lecture Notes in Physics 564. Berlin: Springer Verlag, (2001)
3. Goldshtein, A., Shapiro, M.: J Fluid Mech, **282**, 41 (1995)
4. Dufty, J.W.: Adv Complex Syst **4**, 397 (2001)
5. van Noije, T.P.C., Ernst, M.H.: In: Granular gases, Pöschel, T., Luding, S.: (ed.) Lecture Notes in Physics 564. Berlin, Heidelberg, New York: Springer, pp. 3–30 (2001)
6. Brey, J.J., Cubero, D.: In Granular gases, Pöschel, T., Luding, S.: Lecture Notes in Physics 564. Berlin, Heidelberg, New York: Springer, pp. 59–78 (2001)
7. Brey, J.J., Dufty, J.W., Santos, A.: J Stat Phys **87**, 1051 (1997)
8. Garzó, V., Dufty, J.W.: Phys Rev E **59**, 5895 (1999)
9. Luding, S., Müller, M., McNamara, S.: In World congress on particle technology, CD: ISBN 0-85295-401-9. Brighton, 1998
10. Luding, S.: In T.A.S.K. Quarterly, Scientific Bulletin of Academic Computer Centre of the Technical University of Gdansk, **2**, 417 (1998)
11. Luding, S.: ZAMM **80**, 9 (2000)
12. Soto, R., Mareschal, M.: Phys Rev E **63**, 041303 (2001)
13. Soto, R., Piasecki, J., Mareschal, M.: Phys Rev E **64**, 031306 (2001)
14. Pagonabarraga, I., Trizac, E., van Noije, T.P.C., Ernst, M.H.: Phys Rev E **65**, 011303 (2002)
15. McNamara, S., Luding, S.: Phys Rev E **58**, 2247 (1998)
16. Luding, S., Strauss, O., McNamara, S.: In: Segregation in granular flows. IUTAM Symposium. Rosato, A.D., Blackmore, D.L. (eds.) Dordrecht: Kluwer Academic, pp. 297–303 (2000)
17. Brey, J.J., Ruiz-Montero, M.J.: Phys Rev E **69**, 011305 (2004)
18. Lutsko, J., Brey, J.J., Dufty, J.W.: Phys Rev E **65**, 051304 (2002)
19. Dahl, S.R., Hrenya, C.M., Garzó, V., Dufty, J.W.: Phys Rev E **66** 041301 (2002)
20. Yang, X., Huan, C., Candela, D., Mair, R.W., Walsworth, R.L.: Phys Rev Lett **88**, 044301 (2002)
21. Huan, C., Yang, X., Candela, D., Mair, R.W., Walsworth, R.L.: Phys Rev E **69**, 041302 (2004)
22. Garzó, V., Dufty, J.W.: Phys Rev E **60**, 5706 (1999)
23. Luding, S., Strauss, O.: In: Granular gases. Pöschel, T., Luding, S.: (eds.) Lecture Notes in Physics 564. Berlin, Heidelberg, New York: Springer, pp. 389–409 (2001)
24. Montanero, J.M., Garzó, V.: Granular Matter **4**, 17 (2002)
25. Barrat, A., Trizac, E.: Granular Matter **4**, 57 (2002)
26. Krouskup, P., Talbot, J.: Phys Rev E **68**, 021304 (2003)
27. Wang, H., Jin, G., Ma, Y.: Phys Rev E **68**, 031301 (2003)
28. Clelland, R., Hrenya, C.M.: Phys Rev E **65**, 031301 (2002)
29. Alam, M., Luding, S.: J Fluid Mech **476**, 69 (2003)
30. Willits, J.T., Arnarson, B.: Phys Fluids **11**, 3116 (1999)
31. Alam, M., Willits, J., Arnarson, B., Luding, S.: Phys Fluids **14**, 4085 (2002)

32. Wildman, R.D., Parker, D.J.: Phys Rev Lett **88**, 064301 (2002)
33. Feitosa, K., Menon, N.: Phys Rev Lett **88**, 198301 (2002)
34. Campbell, C.S.: Annu Rev Fluid Mech **22**, 57 (1990)
35. Goldhirsch, I.: Annu Rev Fluid Mech **35**, 267 (2003)
36. In the case of a monocomponent system, see for instance, Lun, C.K.K., Savage, S.B., Jeffrey, D.J., Chepurniy, N.: J Fluid Mech **140**, 223 (1984)
37. Jenkins, J.T., Richman, M.W., J Fluid Mech **192**, 313 (1988)
38. Campbell, C.S.: J Fluid Mech **203**, 449 (1989)
39. Hopkins, M.A., Shen, H.H.: J Fluid Mech **244**, 477 (1992)
40. Lun, C.K.K., Bent, A.A.: J Fluid Mech **258**, 335 (1994)
41. Goldhirsch, I., Tan, M.L.: Phys Fluids **8**, 1752 (1996)
42. Brey, J.J., Ruiz-Montero, M.J., Moreno, F.: Phys Rev E **55**, 2846 (1997)
43. Chou, C.-S., Richman, M.W.: Physica A **259**, 430 (1998)
44. Garzó, V., Santos, A.: Kinetic theory of gases in shear flows. Nonlinear transport. Dordrecht: Kluwer Academic, 2003
45. Alam, M., Luding, S.: Phys Fluids, **17**, 063303 (2005)
46. Lees, A.W., Edwards, S.F.: J Phys C **5**, 1921 (1972)
47. Allen, M.P., Tildesley, D.J.: Computer simulation of liquids. New York: Oxford University Press, 1989
48. Tij, M., Tahiri, E., Montanero, J.M., Garzó, V., Santos, A., Dufty, J.W.: J Stat Phys **103**, 1035 (2001)
49. Garzó, V., Montanero, J.M.: Phys Rev E **68**, 041302 (2003)
50. Santos, A., Garzó, V., Dufty, J.W.: Phys Rev E **69**, 061303 (2004)
51. Dufty, J.W., Santos, A., Brey, J.J., Rodríguez, R.F.: Phys Rev A **33**, 459 (1986)
52. Montanero, J.M., Garzó, V.: Physica A **310**, 17 (2002)
53. Montanero, J.M., Garzó, V.: Mol Sim **29**, 357 (2003)
54. Garzó, V., Montanero, J.M.: Granular Matter **5**, 165 (2003)
55. Chapman, S., Cowling, T.G.: The mathematical theory of nonuniform gases. Cambridge: Cambridge University Press, 1970
56. Lutsko, J.: Phys Rev E **70**, 061101 (2004)
57. Bird, G.A.: Molecular gas dynamics and the direct simulation monte carlo of gas flows. Oxford: Clarendon, 1994
58. Montanero, J.M., Santos, A.: Phys Rev E **54**, 438 (1996) Phys Fluids **9**, 2057 (1997)
59. Müller, M., Luding, S., Herrmann, H.J.: In: Friction, arching and contact dynamics. Wolf, D., Grassberger, P. Singapore: World Scientific, 1997
60. Herrmann, H.J., Müller, M.: Comput Phys Commun **127**, 120 (2000)
61. Montanero, J.M., Garzó, V., Santos, A., Brey, J.J.: J Fluid Mech **389**, 391 (1999)
62. Alam, M., Luding, S.: Phys Fluids **15**, 2298 (2003)
63. Alam, M., Luding, S.: In: Powders & Grains. Garcia-Rojo, R., Herrmann, H.J., McNamara, S.: (eds.) The Netherlands: Balkema Publishers, pp. 1181–85 (2005)
64. Alam, M., Luding, S.: Granular Matter **4**, 139 (2002)
65. Jenkins, J.T., Mancini, F.: J Appl Mech **54**, 27 (1987)
66. Luding, S., Santos, A.: J Chem Phys **121**, 8458 (2004)
67. Boublik, T.: J Chem Phys **53**, 471 (1970)
68. Grundke, E.W., Henderson, D.: Mol Phys **24**, 269 (1972)